

Original Article

Decolorization of direct scarlet 4BS dye using biosynthesized iron nanoparticles as effective heterogeneous Fenton-like catalyst

Natkanin Supamathanon* and Sudarat Sombatsri

*Department of Applied Chemistry, Faculty of Sciences and Liberal Arts,
Rajamangala University of Technology Isan, Mueang, Nakhonratchasima 30000 Thailand*

Received: 7 December 2017; Revised: 1 August 2018; Accepted: 6 September 2018

Abstract

In the present study, iron nanoparticles (Fe-NPs) were synthesized using extracts of green tea leaves as reducing and capping agents under atmospheric conditions. The Fe-NPs were characterized using scanning electron microscopy, energy-dispersive spectrometry, transmission electron microscopy, X-ray diffraction, and Fourier transform infrared spectroscopy. The nanoparticles were mostly spherical and uniform in size with diameters that ranged from 50 to 70 nm and then used as a Fenton-like catalyst for the decolorization of direct scarlet 4BS in solution. About 85% of the dye was successfully removed in 30 min using 1 g/L of catalyst in the presence of 15 mM of H₂O₂ at low (acidic) pH values of 2–4 at room temperature.

Keywords: green synthesis, iron nanoparticles, direct scarlet 4BS, Fenton-like catalyst

1. Introduction

Nowadays, the pollution of water sources by dyes from many industries such as textile, paper, plastic, food, and pharmaceutical are still a major threat to the environment (Forgacs, Cserháti & Oros, 2004). The release of dye effluents into water sources causes serious impact on the aquatic organisms by hindering sunlight into the water. Therefore, it is necessary to treat the water containing these dyes. Conventional water treatment methods include chemical coagulation, flocculation, chemical oxidation, photochemical degradation, membrane filtration, and aerobic and anaerobic biological degradation (Khehra, Saini, Sharma, Chadha, & Chimni, 2006; Lin & Peng, 1994; Robinson, McMullan, Marchant, & Nigam, 2011; Tisa, Abdul Raman, & Ashri Wan Daud, 2014). All of these methods are known to be effective; however, their techniques have one or more limitations and none of them are successful in completely removing the colors from wastewater. In recent years, nanocatalysis has emerged as an alternative to conventional water treatment methods. The high effectiveness of a nanocatalyst is due to its high surface area and surface reactivity. Among the metal

nanoparticles, iron nanoparticles (Fe-NPs) are widely used for the effective removal of dye contaminants. Fe-NPs can be synthesized by chemical and biogenic methods. Chemical methods involve the use of toxic chemicals and reaction conditions which lead to chemical toxicity and environmental pollution. The biogenic methods are considered to be safer alternatives to chemical methods of nanosynthesis due to ease, eco-friendly nature, and cost effectiveness (Kumar, Mandal, Kumar, Reddy & Sreedhar, 2013; Machado *et al.*, 2013; Shahwan *et al.*, 2011; Smuleac, Varma, Sikdar & Bhat tacharyya, 2011; Wang, Jin, Chen, Megharaj, & Naidu, 2014). The components in plant extracts, such as polyphenols, flavonoids, and alkaloids which serve as reducing and capping agents, may assist in designing nanomaterials (Iravani, 2011).

Polyphenols are the major component of green tea extract (Truskewycz, Shukla & Ball, 2016). Polyphenols from green tea reduce the iron salts to form iron nanoparticles and also cap the metal, thereby protecting it from oxidation. The use of green tea polyphenols to generate Fe-NPs has been examined in the context of *in vitro* biocompatibility (Nadagouda, Castle, Murdock, Hussain & Varma, 2010). Recently, the synthesis of Fe-NPs using green tea extract has been used as a Fenton-like catalyst for the oxidation of bromothymol blue (Hoag *et al.*, 2009), cationic (methylene blue) and anionic (methyl orange) dyes (Shahwan *et al.*, 2011), azo (DR80, Direct Red 80) and anthraquinone (RBB-

*Corresponding author

Email address: nsupamathanon@gmail.com

R, Ramazol Brilliant Blue R) dye mixtures (Truskewycz *et al.*, 2016), and monochlorobenzene (Kuang, Wang, Chen, Megharaj, & Naidu, 2013). The objectives of this research were to study the synthesis of Fe-NPs in green tea leaf extract and to investigate the effectiveness of Fe-NPs as a Fenton-like catalyst for decolorizing direct scarlet 4BS from synthetic wastewater.

2. Materials and Methods

2.1 Chemicals

Direct scarlet 4BS dye (4BS) was received from PKS Chemical Co. Ltd., Thailand. Green tea leaves were obtained from Baichachokchamroen Co. Ltd., Thailand. The chemical structures are illustrated in Figure 1. All chemicals, such as hydrogen peroxide (H₂O₂, 35% w/v), sulfuric acid (H₂SO₄), and ferrous sulfate heptahydrate (FeSO₄·7H₂O) were analytical reagent grade.

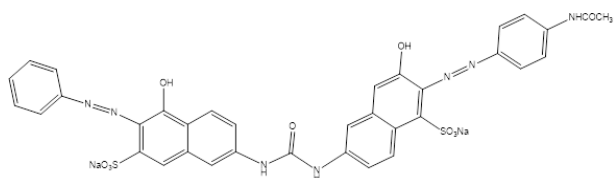


Figure 1. Chemical structure of direct scarlet 4BS.

2.2 Preparation of Fe-NPs

The green tea extract was prepared by heating 60.0 g/L green tea leaves until boiling. After settling for 1.0 h, the extract was filtered. Finally, the tea extract was obtained. Separately, a solution of 0.10 M FeSO₄·7H₂O was added to the green tea extract in 2:1 volume ratio at room temperature. The immediate appearance of a black color indicated the reduction of Fe²⁺ ions. These precipitates were then filtered and centrifuged. The resulting Fe-NPs were washed with distilled water at least 3 times and then dried in a vacuum oven. Finally, the solid Fe-NPs were collected.

2.3 Characterization of the Fe-NPs

The synthesized Fe-NPs were characterized using X-ray diffraction (XRD), transmission electron microscopy (TEM), scanning electron microscopy (SEM)/energy-dispersive spectrometry (EDS), and Fourier transform infrared spectroscopy (FTIR) techniques. Morphology of the Fe-NPs was observed using SEM (SEM-JEOL-JSM-7800F) and elements in the Fe-NPs were determined using EDS (Oxford ED2000). TEM images were obtained from a JEOL JEM-2010 microscope. The crystalline structure of the Fe-NPs was analyzed by XRD (Bruker D2 PHASER) using CuK_α radiation at 30 kV and 10 mA. Data were collected from 10° to 80° with a step size of 0.02. FTIR spectroscopy spectra were obtained using a Perkin Elmer Spectrum 100 FTIR spectrometer. Thermogravimetric analysis of the produced nanoparticles was done on a thermogravimetric analyzer (STA 6000, Perkin Elmer) under nitrogen atmosphere at the heating rate of 10 °C/min in the range of 30–700 °C.

2.4 Decolorization experiments

All experiments were carried out in 125 mL-Erlenmeyer flasks with 50 mL of 50 mg/L 4BS. The pH of the solutions was adjusted to the desired values using 2.0 M H₂SO₄ and after that the Fe-NPs were added. The reactions were initiated by adding a predetermined amount of H₂O₂ solution to the flask. The mixture solution was stirred with a magnetic stirrer. At a regular interval of time, 1 mL of the reaction mixture was withdrawn and centrifuged immediately to remove the catalyst. The concentrations of 4BS were measured using a double beam UV-vis spectrophotometer (Shimadzu, model UV 1601, Japan) at 504 nm. The decolorization efficiency of the 4BS was calculated using the following equation:

$$\text{Decolorization efficiency (\%)} = \frac{C_0 - C_t}{C_0} \times 100$$

where C₀ (mg/L) is the initial concentration of 4BS and C_t (mg/L) is the concentration of 4BS at time t in minutes.

3. Results and Discussion

3.1 Characterization of the Fe-NPs

The SEM and TEM images of the synthesized Fe-NPs are shown in Figure 2(a)–(b). It is clearly seen that the Fe-NPs have a spherical shape. The TEM image as seen in the polyphenol capping agent indicated successful production of the Fe-NPs nanohybrids. The size distribution of the particles is shown in Figure 2(c). The average size of the particles was found to be about 63 nm and the size of the nanoparticles varied in the range of 30–100 nm.

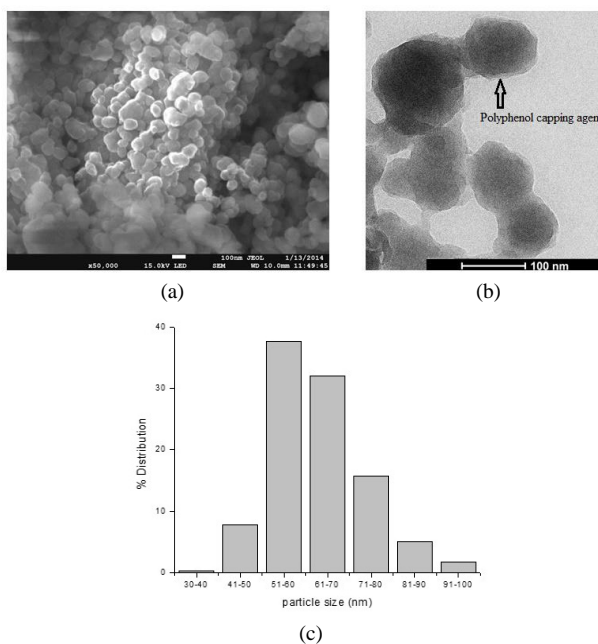


Figure 2. (a) SEM image, (b) TEM image, and (c) particle size distribution of the Fe-NPs.

Figure 3 shows a representative EDX spectrum of the iron nanoparticles. The iron nanoparticles were composed primarily of C, N, O, P, and Fe. The C and O elements originated predominantly from the phytochemicals (phenolic and flavonoid compounds) (Kuang *et al.*, 2013; Quideau, Deffieux, Douat-Casassus, & Pouysegu, 2011).

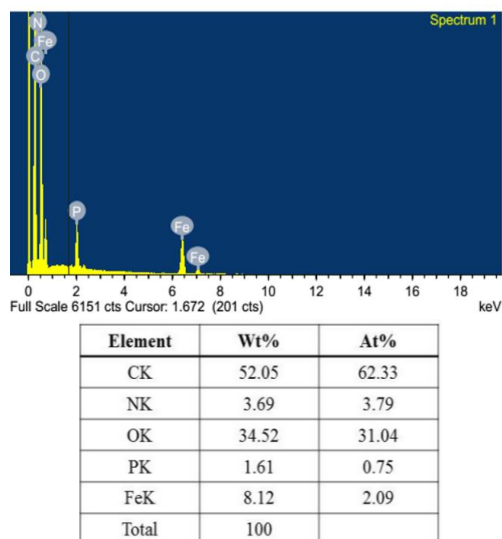


Figure 3. EDX spectrum of the Fe-NPs.

The XRD patterns of the Fe-NPs samples synthesized by green tea plant extracts are shown in Figure 4(a). The patterns of the Fe-NPs samples lack distinct diffraction peaks which suggest that the Fe-NPs are amorphous. The broad peaks at about $2\theta = 25^\circ$ can be attributed to organic materials from the plant extract which are responsible for capping and stabilizing the nanoparticles (Kumar *et al.*, 2013; Njagi *et al.*, 2011; Wang, 2013). A similar observation was noticed in the green synthesis of Fe-NPs using extracts of eucalyptus, *S. jambos* (*L.*) *Alston* and sorghum bran (Njagi *et al.*, 2011; Xiao *et al.*, 2016; Wang, 2014). Figure 4(b) shows the FTIR spectrum of the Fe-NPs and green tea extract. For the extract of green tea, strong bands at 3402 cm^{-1} are assigned to O-H stretching vibrations (Kumar *et al.*, 2013). The peak at 2929 cm^{-1} is characteristic of aliphatic C-H stretching vibrations. The presence of bands were attributed to polyphenolic compounds at 1631 cm^{-1} due to C=C aromatic ring stretching vibration, at 1367 cm^{-1} due to C-N stretching vibration of aromatic amines, and at 1043 cm^{-1} for C-N stretching vibration of aliphatic amines (Das, Borthakur & Bora, 2010). Thus, the functional groups, including phenols, amines, and carboxyl, were confirmed in the green tea. Meanwhile, the FTIR spectrum of the prepared Fe-NPs also displayed stretching vibrations at 3382 cm^{-1} for O-H, at 1630 cm^{-1} for C=C, and $1,068\text{ cm}^{-1}$ for C-O-C absorption peak (Kumar *et al.*, 2013). The FTIR analysis observed some minor shifts in the position of various peaks compared with the green tea extract which indicated the involvement of the plant extract in the synthesis and stabilization of the nanoparticles. Zero-valent iron nanoparticles exhibited a typical core-shell structure. Zero-valent iron atoms form the core which is surrounded by an oxide

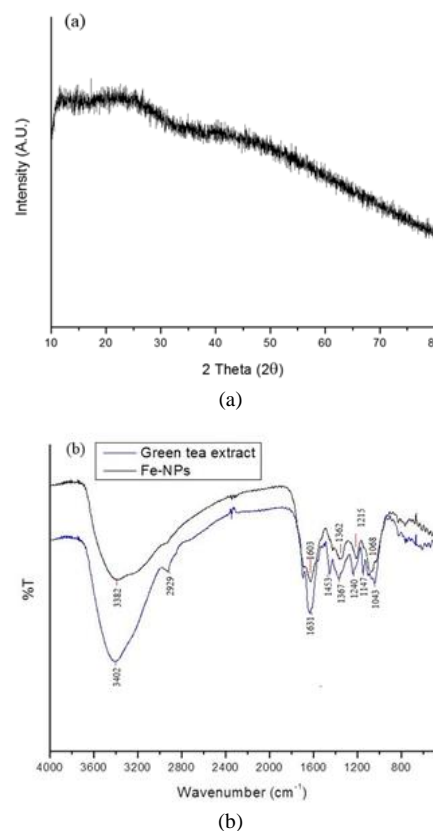


Figure 4. (a) XRD patterns and (b) FTIR spectra of the Fe-NPs and the green tea extract.

shell composed of Fe^{2+} and Fe^{3+} which is formed as a result of the oxidation of the metallic iron (Kharisov *et al.*, 2016). The thin iron oxide shell results in the appearance of Fe-O absorption bands, but at a lower intensity than is usually observed for iron oxide nanoparticles. The Fe-O characteristic peaks of the iron oxide nanoparticles appeared at about 640 cm^{-1} and 450 cm^{-1} (Ebrahimezhad, Ghasemi, Rasoul-Amini, Barar, & Davara, 2012). These peaks were not observed in the FTIR spectrum of the prepared Fe-NPs which indicated the absence of an iron oxide shell. This confirmed that the organic coating from the leaf extract seems to protect the surface of the Fe^0 atoms from oxidation.

The thermogravimetric analysis of the Fe-NPs is shown in Figure 5. The initial weight loss observed prior to $200\text{ }^\circ\text{C}$ relates to the presence of volatile (water and carbon) on the surface of the synthesized Fe-NPs. Beyond $200\text{ }^\circ\text{C}$ the rapid weight loss at high temperatures was possibly due to the decomposition of the phytomolecules from the green tea extract which are present on the surface of the nanoparticles acting as stabilizing agents (Katithi *et al.*, 2016).

3.2 Decolorization experiments

To investigate their catalytic activity, the iron nanoparticles were employed in the decolorization of 4BS in the presence of H_2O_2 . The progress of the catalytic decolorization of 4BS was monitored by a decrease in the absorbance at the maximum absorbance wavelength of 4BS.

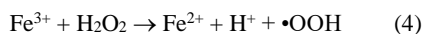
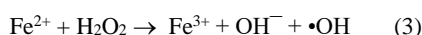
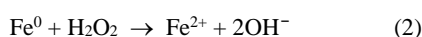
Figure 6 shows the UV-vis spectra of the decolorization of 4BS. The maximum absorbance wavelength (λ_{\max}) of 4BS was at 504 nm and absorbance at 250 and 310 nm confirmed the phenyl and naphthyl rings in the 4BS structure (He, Hu, & Li, 2004). After 10 min of reaction, the dye structure changed markedly and the absorbance at 504 nm disappeared. This occurred due to cleavage of the azo bonds (N=N). However, iron nanoparticles were not stable under acidic pH conditions of 2–4 or in the presence of 15 mM H_2O_2 . The solutions developed a brown-yellow color because the particle size of the zero-valent iron nanoparticles decreased and were well dispersed in the acidic media. The UV-vis spectrum of the brown-yellow solution showed peaks at 272 nm which confirmed the presence of iron nanoparticles (Huang, Weng, Chen, Z. Megharaj, & Naidu, 2014) (Figure 6).

The reaction is based on the action of hydroxyl radicals ($\bullet\text{OH}$) generated in an aqueous solution by the well-known Fenton reagent which is a combination of Fe^{2+} and H_2O_2 in an aqueous solution for the oxidation of organic pollutants from contaminated water. Based on the above results, a possible mechanism for Fenton-like degradation of the 4BS dye employing Fe-NPs has been proposed and was similarly reported by Kuang *et al.* (2013), in Equations 1–6. First, the adsorption of 4BS onto the surface of Fe-NPs occurs (Equation 1). Second, the process of generating hydroxyl radicals is suggested. In the presence of H_2O_2 , the Fe^0 is transformed into Fe^{2+} (Equation 2). Fe^{2+} can then react with H_2O_2 to form $\bullet\text{OH}$ (Equation 3). During the reaction Fe^{3+} is formed which can react to produce Fe^{2+} (Bergendahl & Thies, 2004) (Equation 4). Finally, the highly oxidative $\bullet\text{OH}$ radicals react rapidly with the adsorbed 4BS and effectively attack the bonds of the dye molecules. Part of the 4BS was mineralized on the surface of the Fe-NPs into CO_2 and H_2O . In conclusion, the possible oxidation mechanism using Fe-NPs is described below:

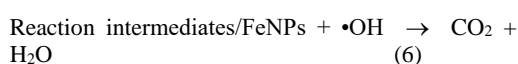
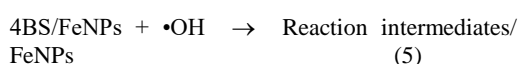
1. Adsorption process:



2. The process of generating $\bullet\text{OH}$ radicals:



3. $\bullet\text{OH}$ radicals attack the 4BS on the surface of the FeNPs:



The decolorization of 4BS was experienced at all four of the pH levels (Figure 7). The greatest decolorization of 4BS occurred at pH levels of 2.0, 3.0, and 4.0 with decolorization of approximately 85% within 30 min. At pH 5.0, the decolorization was 71% within 30 min and the

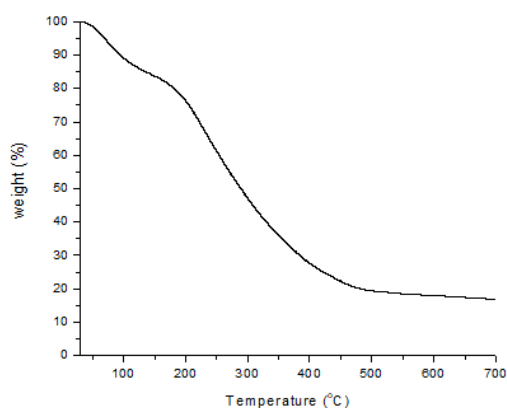


Figure 5. Thermogravimetric analysis curve (% weight loss) of the Fe-NPs.

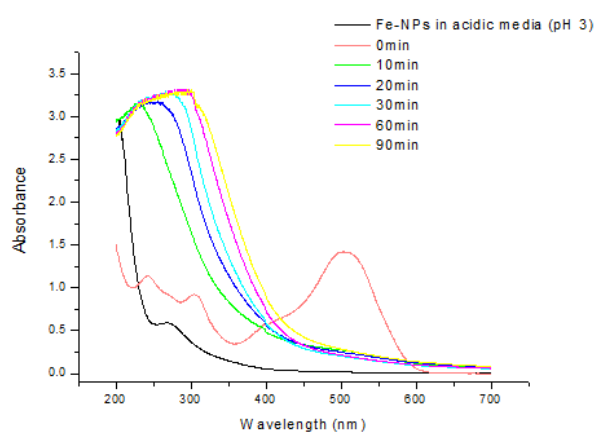


Figure 6. UV-vis absorption spectra of Fe-NPs in media acid solution and 4BS before and after the Fenton-like reaction. Reaction conditions: initial concentration of 4BS, $[\text{4BS}]_0 = 50 \text{ mg/L}$, initial concentration of hydrogen peroxide, $[\text{H}_2\text{O}_2]_0 = 15 \text{ mM}$, catalyst amount = 1.0 g/L , initial pH = 3, and temperature = $26 \text{ }^\circ\text{C}$.

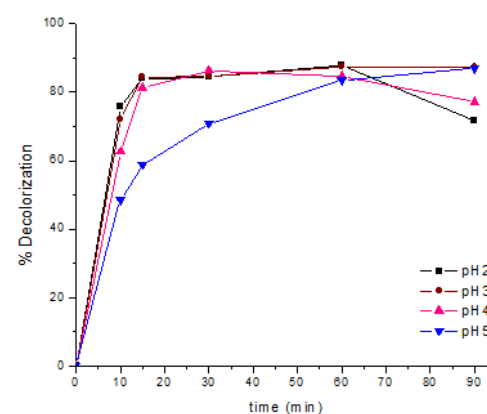


Figure 7. Effect of pH on the decolorization of 4BS. Reaction conditions: initial concentration of 4BS, $[\text{4BS}]_0 = 50 \text{ mg/L}$, initial concentration of hydrogen peroxide, $[\text{H}_2\text{O}_2]_0 = 15 \text{ mM}$, catalyst amount = 1.0 g/L , and temperature = $26 \text{ }^\circ\text{C}$.

decolorization was up to approximately 83% at increased reaction time. It can be concluded that the optimum for the Fenton oxidation falls mostly in the lower acidic pH range because a high amount of Fe^{2+} and $\bullet\text{OH}$ was generated (Bergendahl & Thies, 2004; Chen, Ma & Sun, 2008; He *et al.*, 2004; Pignatello, Oliveros, & MacKay, 2006). The effect of H_2O_2 on the decolorization of 4BS was examined by varying the initial concentration of H_2O_2 from 7 to 28 mM at pH 3.0 (Figure 8). The best initial H_2O_2 concentration was obtained at 15 mM. Decolorization of 4BS increased as the concentration of H_2O_2 increased due to the high concentration of $\bullet\text{OH}$ radical generation to catalyze the organic dye. However, the formation of less reactive species such as hydroperoxyl radicals ($\bullet\text{OOH}$) may be generated due to the scavenging effect of hydroxyl radicals and the inhibition of iron corrosion on the surface of Fe-NPs by H_2O_2 (Equation 7) with the increase of the reaction time when an initial concentration of 28 mM H_2O_2 was used (Kuang *et al.*, 2013).

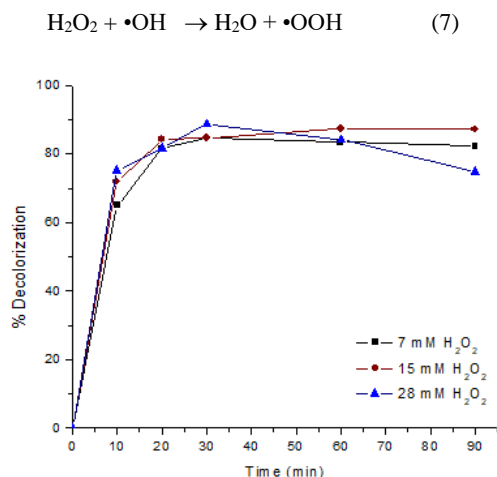


Figure 8. Effect of initial concentration of H_2O_2 on the decolorization of 4BS. Reaction conditions: initial concentration of 4BS, $[\text{4BS}]_0 = 50 \text{ mg/L}$, initial pH = 3, catalyst amount = 1.0 g/L , and temperature = $26 \text{ }^\circ\text{C}$.

4. Conclusions

Iron nanoparticles were successfully synthesized using a green tea leaf extract following the green procedure. The phytochemicals in the leaf extract play dual roles as both are reducing and stabilizing agents. The Fe-NPs showed a sphere-like morphology. Furthermore, the Fe-NPs exhibited good catalytic effects on the decolorization of the 4BS dye with H_2O_2 based on the Fenton-like reaction. The results show that the green synthesis of Fe-NPs can be an effective technology for treating wastewater containing organic dyes.

Acknowledgements

The authors would like to thank the Department of Applied Chemistry, Faculty of Sciences and Liberal Arts, Rajamangala University of Technology Isan, for providing of the research facilities. Asst. Prof. Dr. Artit Ausavasukhi is acknowledged for data discussion.

References

- Bergendahl, J. A., & Thies, T. P. (2004). Fenton's oxidation of MTBE with zero-valent iron. *Water Research*, 38(2), 327-334. doi:10.1016/j.watres.2003.10.003
- Chen, A., Ma, X., & Sun, H. (2008). Decolorization of KN-R catalyzed by Fe containing Y and ZSM-5 zeolites. *Journal of Hazardous Materials*, 156(1-3), 568-575. doi:10.1016/j.jhazmat.2007.12.059
- Das, R. K., Borthakur, B. B., & Bora, U. (2010). Green synthesis of gold nanoparticles using ethanolic leaf extract of *Centella asiatica*. *Materials Letters*, 64(13), 1445-1447. doi:10.1016/j.matlet.2010.03.051
- Ebrahiminezhad, A., Ghasemi, Y., Rasoul-Amini, S., Barar, J., & Davara, S. (2012). Impact of amino-acid coating on the synthesis and characteristics of Iron-Oxide Nanoparticles (IONs). *Bulletin of the Korean Chemical Society*, 33(12), 3957-3962. doi:10.5012/bkcs.2012.33.12.3957
- Forgacs, E., Cserhati, T., & Oros, G. (2004). Removal of synthetic dyes from wastewaters: A review. *Environment International*, 30(7), 953-971. doi:10.1016/j.envint.2004.02.001
- He, F., Hu, W., & Li, Y. (2004). Biodegradation mechanisms and kinetics of azo dye 4BS by a microbial consortium. *Chemosphere*, 57(4), 293-301. doi:10.1016/j.chemosphere.2004.06.036
- Hoag, G. E., Collins, J. B., Holcomb, J. L., Hoag, J. R., Nadagouda, M. N., & Varma, R. S. (2009). Degradation of bromothymol blue by 'greener' nano-scale zero-valent iron synthesized using tea polyphenols. *Journal of Materials Chemistry*, 19, 8671-8677. doi: 10.1039/b909148c
- Huang, L., Weng, X., Chen, Z., Megharaj, M. & Naidu, R. (2014). Green synthesis of iron nanoparticles by various tea extracts: Comparative study of the reactivity. *Spectrochimica Acta Part A: Molecular and Biomolecular Spectroscopy*, 130, 295-301. doi:10.1016/j.saa.2014.04.037
- Iravani, S. (2011). Green synthesis of metal nanoparticles using plants. *Green Chemistry*, 13, 2638-2650. doi:10.1039/C1GC15386B
- Katithi, D. M., Michira, I. N., Guto, P. M., Baker, P., Kamau, G. N., & Iwuoha, E. (2016). Synthesis and characterization of green tea stabilized iron nanocatalysts for bromothymol blue (BTB) degradation. *Journal of Nano Research*, 42, 1-13. doi:10.4028/www.scientific.net/JNanoR.42.1
- Kharisov, B. I., Kharissova, O. V., Rasika Dias, H. V., Ortiz Mendez, U., Gomez De La Fuente, I., Pena, Y., Norena, L. E., & Vazquez Dimas, A. (2016). Iron-based nanomaterials in the catalysis. *Intech*, 35-68. doi:10.5772/61862
- Khehra, M. S., Saini, H. S., Sharma, D., Chadha, B. S., & Chimni, S. S. (2006). Biodegradation of azo dye C.I. Acid red 88 by an anoxic-aerobic sequential bio-reactor. *Dyes and Pigments*, 70(1), 1-7. doi:10.1016/j.dyepig.2004.12.021
- Kuang, Y., Wang, Q., Chen, Z., Megharaj, M., & Naidu, R. (2013). Heterogeneous Fenton-like oxidation of monochlorobenzene using green synthesis of iron

- nanoparticles. *Journal of Colloid and Interface Science*, 410, 67-73. doi:10.1016/j.jcis.2013.08.020
- Kumar, K. M., Mandal, B. K., Kumar, K. S., Reddy, P. S., & Sreedhar, B. (2013). Biobased green method to synthesise palladium and iron nanoparticles using Terminalia chebula aqueous extract. *Spectrochimica Acta Part A: Molecular and Biomolecular Spectroscopy*, 102, 128-133. doi:10.1016/j.saa.2012.10.015
- Lin, S. H., & Peng, C. F. (1994). Treatment of textile wastewater by electrochemical method. *Water Research*, 28(2), 277-282. doi:10.1016/0043-1354(94)90264-X
- Machado, S., Pinto, S. L., Grosso, J. P., Nouws, H. P. A., Albergaria, J. T., & Delerue-Matos, C. (2013). Green production of zero-valent iron nanoparticles using tree leaf extracts. *Science of the Total Environment*, 445-446, 1-8. doi:10.1016/j.scitotenv.2012.12.033
- Nadagouda, M. N., Castle, A. B., Murdock, R. C., Hussain, S. M., & Varma, R. S. (2010). In vitro biocompatibility of nanoscale zerovalent iron particles (NZVI) synthesized using tea polyphenols. *Green Chemistry*, 12, 114-122. doi:10.1039/b921203p
- Njagi, E. C., Huang, H., Stafford, L., Genuino, H., Galindo, H. M., Collins, J. B., Hoag, G. E., & Suib, S. L. (2011). Biosynthesis of iron and silver nanoparticles at room temperature using aqueous sorghum bran extracts. *Langmuir*, 27(1), 264-271. doi:10.1021/la103190n
- Pignatello, J. J., Oliveros, E., & MacKay, A. (2006). Advanced oxidation processes for organic contaminant destruction based on the Fenton reaction and related chemistry. *Critical Reviews in Environmental Science and Technology*, 36, 1-84. doi:10.1080/10643380500326564
- Quideau, S., Deffieux, D., Douat-Casassus, C., & Pouysegue, L. (2011). Plant polyphenols: Chemical properties, biological activities, and synthesis. *Angewandte Chemie International Edition*, 50, 586-621. doi:10.1002/anie.201000044
- Robinson, T., McMullan, G., Marchant, M., & Nigam, P. (2001). Remediation of dyes in textile effluent: A critical review on current treatment technologies with a proposed alternative. *Bioresource Technology*, 77(3), 247-255. doi:10.1016/S0960-8524(00)00080-8
- Shahwan, T., Abu Sirriah, S., Nairat, M., Boyaci, E., Eroglu, A. E., Scott, T. B., & Hallam, K. R. (2011). Green synthesis of iron nanoparticles and their application as a Fenton-like catalyst for the degradation of aqueous cationic and anionic dyes. *Chemical Engineering Journal*, 172(1), 258-266. doi:10.1016/j.cej.2011.05.103
- Smuleac, V., Varma, R., Sikdar, S., & Bhattacharyya, D. (2011). Green synthesis of Fe and Fe/Pd bimetallic nanoparticles in membranes for reductive degradation of chlorinated organics. *Journal of Membrane Science*, 379(1-2), 131-137. doi:10.1016/j.memsci.2011.05.054
- Tisa, F., Abdul Raman A. A., & Ashri Wan Daud, W. M. (2014). Applicability of fluidized bed reactor in recalcitrant compound degradation through advanced oxidation processes: A review. *Journal of Environmental Management*, 146, 260-275. doi:10.1016/j.jenvman.2014.07.032
- Truskewycz, A., Shukla, R. & Ball A.S. (2016). Iron nanoparticles synthesized using green tea extracts for the fenton-like degradation of concentrated dye mixtures at elevated temperatures. *Journal of Environmental Chemical Engineering*, 4, 4409-4417. doi:10.1016/j.jece.2016.10.008.
- Wang, T., Jin, X., Chen, Z., Megharaj, M., & Naidu, R. (2014). Green synthesis of Fe nanoparticles using eucalyptus leaf extracts for treatment of eutrophic wastewater. *Science of The Total Environment*, 466-467, 210-213. doi:10.1016/j.scitotenv.2013.07.022
- Wang, Z. (2013). Iron complexes nanoparticles synthesized by eucalyptus leaves. *ACS Sustainable Chemistry and Engineering*, 1(12), 1551-1554. doi:10.1021/sc400174a
- Xiao, Z., Yuan, M., Yang, B., Liu, Z., Huang, J., & Sun, D. (2016). Plant-mediated synthesis of highly active iron nanoparticles for Cr (VI) removal: Investigation of the leading biomolecules. *Chemosphere*, 150, 357-364. doi:10.1016/j.chemosphere.2016.02.056